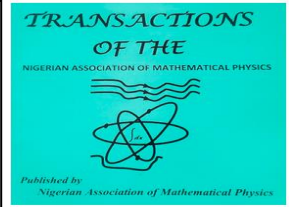


**Transactions of
The Nigerian Association of
Mathematical Physics**
Journal homepage: <https://nampjournals.org.ng>



NAVIER SLIP AND CONVECTIVE BOUNDARY CONDITION EFFECTS ON TRANSIENT COMBINED CONVECTION OF DISSIPATIVE FLUID

Muhammed Murtala Hamza¹, Yakubu Bello² and Samaila Kenga-kwai Ahmad³

^{1,3}Department of Mathematics, Faculty of Physical and Computing Science, Usmanu Danfodiyo University, Sokoto State, Nigeria.

²Department of Mathematics, Faculty of Science, Air Force Institute of Technology, P.M. B. 2104, Kaduna State, Nigeria.

ARTICLE INFO

Article history:

Received xxxxx

Revised xxxxx

Accepted xxxxx

Available online xxxxx

Keywords:

Navier Slip,

Viscos Dissipation,

Homotopy perturbation,

Convective Boundary.

ABSTRACT

This research aims to investigate the unsteady behavior of Navier slip and convective boundary condition on transient mixed convection flow of a viscous dissipative fluid in a vertical channel. To get steady state solutions for temperature and velocity distributions, the Homotopy Perturbation Techniques (HPM) is applied. Numerical solutions of the transient leading equations is performed using the implicit finite difference scheme. Tables and graphs are used to display the dynamic flow parameters. Numerical analysis demonstrates that, increasing the parameters for the Darcy parameter (Da), Biot number (Bii) and mixed convection parameter (Gre) all resulted in an upward flow of fluid, however increasing the parameters for the heat sink and magnetic field resulted in a downward flow of fluid.

1.0 INTRODUCTION

In a wide variety of circumstances, free convection coexists with mixed convection due to forces of comparable strength. Such type of flow can be found in isothermal flows, slow flows through tubes (e.g. water radiators) or along walls and atmospheric flows. According to Avci and Aydin [1] and Avramenko [2], mixed convection in micro-channels has been used for many years to treat heat transfer. This led Jha et al. [3] to conduct a theoretical analysis on a fully developed hydro-magnetic fluid in a vertical micro-channel that emits, absorbs, and is impacted by Hall and ion-slip phenomena. When there is obvious heat generation and absorption, increases in ion-slip and hall current parameters can increase primary velocity and temperature gradient. Khanafer et al. [4] reported mixed convection heat transfer in a differentially heated cylinder speed depression across an opposing-moving channel is examined. They discovered that the average Nusselt number rises in response to increased Reynolds, Richardson, and cylinder rotating speeds. This model also shows that at large Richardson numbers, the heat transmission rate was comparable to the cylinder speed ethics. According to Gupta et al. [5], an increase in the Grashof number, the suction parameter, and the permeability parameter causes a fluid's velocity to rise. In contrast, a rise in the thermal gradient is caused by an increase in the magnetic

*Corresponding author: Muhammed M.H.

E-mail address: muhammed.hamza@udusok.edu.ng

<https://www.doi.org/10.60787/tnamp-19-167-178>

1118-4752 © 2024 TNAMP. All rights reserved

parameter and the dissipating parameter. A decrease in the suction parameter or Prandtl number causes a rise in the thermal gradient. Masoud et al. [6] conducted an experimental study to determine the MWCNT-CuO/water nanofluid's thermal conductivity. A theoretical examination of a hybrid nanofluid in a vertical micro channel with mixed convection was presented by Xu and Sun [7]. They asserted that the nanoparticle volumetric fractions had a major impact on the dynamic and thermal behaviors. Additionally, they demonstrated how the volume proportions of Ri and nanoparticles would increase the average heat transmission rate. Manay and Mandev [8] investigated the mixed convection of nano-fluids in spherical micro-channels. They found that the rate of heat transmission increased as the fraction of silicon dioxide nanoparticles in suspension increased.

The study of viscous dissipation in both free and mixed convections has catalyzed a variety of interesting investigations because it would get smaller independent of the Reynolds number, and because of its potential applications in lubricating industries, nuclear reactor cooling, electric appliance cooling, and so on. Viscous dissipation is a crucial characteristic that happens when fluid particles contact and produce internal mechanical energy. In terms of fluid hydrodynamics and thermodynamics, this kind of energy dissipation has significant consequences. Viscous dissipation in the lubricating sector is inevitable. The first person to examine how viscous dissipation affects natural convection was Gebhart [9]. He discovered that viscous dissipation in a fluid with a high Prandtl number or a fluid with strong gravitational forces cannot be disregarded in a steady state of natural convection. Since then, several researchers have looked at heat transfer in a variety of geometries using combined convection and viscous dissipation in fluids that generate and absorb heat. In this context, Ajibade and Umar [10] published an analytical analysis of the impact of a constant hydro-magnetic free convection flow on heat-generating and -absorbing fluid along with viscous dissipation. Following up on their earlier research, Ajibade and Umar [11] used the homotopy perturbation method to examine the effects of viscous dissipation and suction/injection on fully developed laminar flow of heat-generating and heat-absorbing fluid through a vertical parallel porous plate passage in a steady MHD mixed convection flow. Jha and Ajibade [12] looked at viscous dissipation and convective heat transmission between vertical parallel plates with a time-periodic boundary layer. They demonstrated that when the fluid's Prandtl number is low, dissipation heating in the channel elevates the fluid's temperature over the plate temperature. The unsteady free convective flow of a heat source or sink was studied by Jha and Ajibade [13]. According to their research, heat transfer rates improve on moving plates when heat absorption rises, whereas they decline on stationary plates. The entropy production and irreversibility analysis of a vertical porous channel with a continuous mixed convection flow were studied by Ajibade and Thomas [14]. In addition to the temperature displaying the opposite tendency, they found that whenever mixed convection increases, so does the velocity profile. Mohamed [15] investigated the role of viscous dissipation in a micro-polar fluid's mixed convection flow on unsteady stretching surface. His findings shown that when the Eckert number rises, temperature and velocity also rise. Mohamed [16] explored on the vertical boundary layer flow of mixed convection heat transfer and viscous dissipation and variable viscosity. He has demonstrated that, compared to unsteady flow, steady flow has greater influence of the mixed convection parameter on fluid acceleration and heat distribution. He also found that the flow and temperature fields grew as the mixed convection parameter's efficacy did. The effects of temperature-dependent viscosity and variable thermal conductivity on the diffusion of non-Darcy mixed convective species in magnetohydrodynamics (MHD) over a stretched surface were examined by Dulal and Hiranmony [17]. They reached the conclusion that the fluid velocity increases as the mixed convection parameter grows while the temperature profile falls because the wall thickness at the thermal barrier decreases as the mixed convection increases.

A method that is becoming more and more popular for enhancing convective thermal behavior is the use of porous media in micro-channels and heat exchangers. A porous media, according to Mahmoodi et al. [18], is a solid matrix containing empty spaces called pores connected by a network of channels that allow fluid to move through. The storage of radioactive nuclear waste, geothermal extraction, transpiration cooling, filtration, crude oil extraction, heating and cooling in buildings, and many more uses for the movement of fluid and heat are only a few instances. Using Hamming's predictor-corrector approach, According to Samaila *et al.* [19], increasing the values of gr , br , and da improves the fluid velocity whereas increasing the values of m and pr has the opposite effect on the flow pattern, in their study of a numerical investigation of hydro-magnetic mixed convection flow of viscous dissipative fluid in a channel filled with porous material, Chamkha [20] employed the Kellerbox approach to examine the non-similar solution of natural convection boundary layer flow over a sphere embedded in a porous medium saturated with nanofluid. Chamkha et al. [21] investigated the impact of a transverse magnetic field on free and forced convection events in a porous material with homogeneous heat flow over a semi-infinite permeable vertical plate. The MHD convection flow of Casson fluid in microchannels with permeable medium was explored by Gireesha and Sindhu [22]. When Noor et al. [23] evaluated time-dependent hydro-magnetic radiative fluid flow over an inclined porous plate with heat and mass conductivity using network simulation method solutions, they found that the fluid momentum continued to rise or fall gradually as it approached the plate and then decreased or grew more slowly as it moved away from the plate. It has been noted that the fluid's temperature displays the similar trend.

This study aims to investigate the effects of Navier slip and convective boundary conditions on transient mixed convection flow of viscous dissipative fluid in a vertical channel. Since the current flow problem's leading equations are coupled and nonlinear, it is challenging to arrive at closed-form solutions. Therefore, numerical methods or approximate solution approaches can be used to overcome these issues. The perturbation technique is one of the most effective processes. However, the perturbation approach can

only find solutions for tiny perturbation parameters. To get around this restriction, the Homotopy perturbation approach emerged. He [24] applied the technique to unravel partial or regular linear, nonlinear, and coupled equations. The study would examine how Navier slip and convective boundary conditions affect transient mixed convection flow of viscous dissipative fluid in a vertical channel. The findings of this study can help designers improve the behavior of mechanical systems by including viscous dissipation and heat transfer through channels, which are used in car piston combustion.

2. Mathematical Formulation

Consider a scenario in which a vertical pair of parallel plates filled with porous material is subjected to a time-dependent, fully developed mixed convection flow of a viscous dissipative and heat generating/absorbing fluid; the fluid's motion is caused by the presence of Navier slip and Newtonian heating at the lower plate. It is assumed that the channel is subject to the effects of the applied magnetic field. Following Ajibade and Umar [10], and Hamza [25], the governing equations in dimensional form can be expressed as follows using the aforementioned supposition:

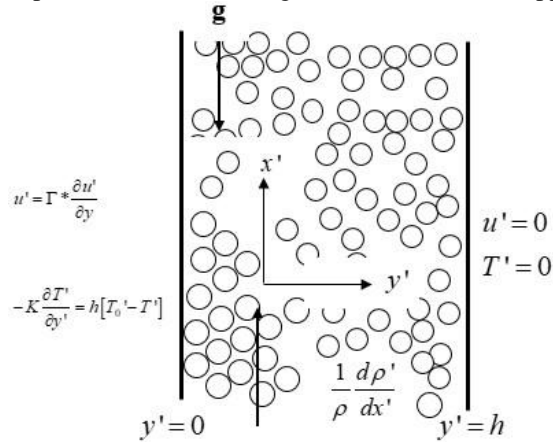


Figure 1. Schematic diagram of the model.

$$\frac{\partial u'}{\partial t} = \nu \frac{\partial^2 u'}{\partial y'^2} + g\beta(T' - T_0) - \frac{\sigma\beta_0}{\rho} u' - \frac{\nu u'}{\kappa} - \frac{1}{\rho} \frac{\partial p'}{\partial x'} \tag{1}$$

$$\frac{\partial T'}{\partial t} = \frac{\kappa}{\rho c_p} \frac{\partial^2 T'}{\partial y'^2} - \frac{Q_0}{\rho c_p} (T' - T_2) + \frac{\nu}{c_p} \left(\frac{\partial u'}{\partial y'} \right)^2 \tag{2}$$

Where y' and x' are the dimensional distances along and perpendicular to the plate. u' and T' are the dimensional velocity, and temperature. $Q_0, \nu, k, \rho, C_p, \beta,$ and g are the dimensional heat source/sink coefficient, kinetic viscosity, thermal conductivity, density, specific heat at constant pressure, thermal expansion coefficient, and acceleration due to gravity of the fluid, respectively. We assume that the appropriate boundary conditions of the model are:

$$\left. \begin{aligned} u' = \Gamma^* \frac{\partial u'}{\partial y'}, \quad -K \frac{\partial T'}{\partial y'} = h[T_0' - T'] \quad \text{at } y' = 0 \\ u' = 0, \quad T' = T_0', \quad \text{at } y' = H \end{aligned} \right\} \tag{3}$$

The following are the dimensionless quantities used:

$$\left. \begin{aligned} u &= \frac{u^*}{U}, \quad y = \frac{y^*}{h}, \quad T = \frac{T^* - T_0}{T_w - T_0}, \quad x = \frac{x^* v}{Uh^2}, \quad P = \frac{p^*}{\rho U^2}, \quad Re = \frac{Uh}{\nu}, \quad Pr = \frac{\nu}{\alpha}, \\ M &= \frac{\sigma \beta_0^2 h^2}{\nu}, \quad Da = \frac{\kappa}{h^2}, \quad \Gamma = \frac{\gamma^*}{H}, \quad Bii = \frac{hH}{K}, \quad Gr = \frac{g\beta(T_w - T_0)h^3}{\nu^2} \\ Ec &= \frac{U^2}{c_p(T_w - T_0)}, \quad Gre = \frac{Gr}{Re}, \quad EcPr = Br, \quad S = \frac{Q_0 h^2}{k} \end{aligned} \right\} \quad (4)$$

where Gr is the thermal Grashof number, Re is the Reynold number, Pr is the Prandtl number, Ec is Eckert number, S is heat source/sink parameter, $\frac{Gr}{Re} = Gre$ is the mixed convection parameter, and $EcPr = Br$ is the Brinkman number.

From the dimensional quantities above, the fundamental field eqn. (1), (2) and (3) can be written in dimensionless form as:

$$\frac{\partial u}{\partial t} = \frac{\partial^2 u}{\partial y^2} + GreT - \left(M + \frac{1}{Da}\right)u - \frac{\partial p}{\partial x} \quad (5)$$

$$Pr \frac{\partial T}{\partial t} = \frac{\partial^2 T}{\partial y^2} + Br \left(\frac{\partial u}{\partial y}\right)^2 - ST \quad (6)$$

And the boundary conditions are:

$$\left. \begin{aligned} u &= \Gamma \frac{\partial u}{\partial y}, & \frac{\partial T}{\partial y} &= -B_{ii} [1-T], & \text{at } y &= 0 \\ u &= 0, & T &= 0, & \text{at } y &= 1 \end{aligned} \right\} \quad (7)$$

By equating $\frac{\partial u}{\partial t} = 0$ and $Pr \frac{\partial T}{\partial t} = 0$

We have

$$\frac{d^2 u}{dy^2} + GreT - \left(M + \frac{1}{Da}\right)u - \frac{dp}{dx} = 0 \quad (8)$$

$$\frac{d^2 T}{dy^2} + Br \left(\frac{du}{dy}\right)^2 - ST = 0 \quad (9)$$

Boundary conditions are:

$$\left. \begin{aligned} u &= \Gamma \frac{du}{dy}, & \frac{dT}{dy} &= -B_{ii} [1-T], & \text{at } y &= 0 \\ u &= 0, & T &= 0, & \text{at } y &= 1 \end{aligned} \right\} \quad (10)$$

3. Methodology

(a) Steady State Solutions

Homotopy Perturbation Method is used to solve the governing equations (8) to (10). Convex homotopy of the momentum and energy equations has been constructed. Therefore, the momentum Eq. (8) is transformed as:

$$H(u, p) = (1-p) \left[\frac{d^2 u}{dy^2} - \frac{d^2 v_0}{dy^2} \right] + p \left[\frac{d^2 u}{dy^2} + GreT - \left(M + \frac{1}{D}\right)u - \frac{dp}{dx} \right] = 0 \quad (11)$$

$$H(u, p) = (1-p) \left[\frac{d^2 T}{dy^2} - \frac{d^2 T_0}{dy^2} \right] + p \left[\frac{d^2 T}{dy^2} + Br \left(\frac{du}{dy}\right)^2 - ST \right] = 0 \quad (12)$$

Since the zeroth order is linear and is solvable without any recourse to initial approximation, therefore, Eq. (8) and (9) can be expressed as:

$$\frac{d^2 u}{dy^2} = p \left[\frac{dp}{dx} + \left(M + \frac{1}{D}\right)u - GreT \right] \quad (13)$$

$$\frac{d^2T}{dy^2} = p \left[ST - Br \left(\frac{du}{dy} \right)^2 \right] \tag{14}$$

Setting velocity (u) and temperature (T) as infinite series such that

$$u = u_0 + pu_1 + P^2u_2 + \dots \tag{15}$$

$$T = T_0 + pT_1 + P^2T_2 + \dots$$

by substituting Eq (15) into Eq (13) and (14), we have

$$\frac{d^2u_0}{dy^2} + p \frac{d^2u_1}{dy^2} + P^2 \frac{d^2u_2}{dy^2} + \dots = p \frac{dP}{dx} + p \left(M + \frac{1}{Da} \right) u_0 + p^2 \left(M + \frac{1}{Da} \right) u_1 + \dots - pGreT_0 - p^2GreT_1 - \dots \tag{16}$$

$$\frac{d^2T_0}{dy^2} + p \frac{d^2T_1}{dy^2} + P^2 \frac{d^2T_2}{dy^2} + \dots = pST_0 + p^2ST_1 + p^3ST_2 + \dots - pBr \left(\frac{du_0}{dy} \right)^2 - 2p^2Br \frac{du_0}{dy} \frac{du_1}{dy} + \dots \tag{17}$$

Comparing the coefficients of p^0, p^1, p^2, \dots , the equation is split as:

$$p^0 : \frac{d^2u_0}{dy^2} = 0 \tag{18}$$

$$p^1 : \frac{d^2u_1}{dy^2} = \frac{dP}{dx} + \left(M + \frac{1}{Da} \right) u_0 - GreT_0 \tag{19}$$

$$p^2 : \frac{d^2u_1}{dy^2} = \left(M + \frac{1}{Da} \right) u_1 - GreT_1 \tag{20}$$

Similarly comparing the coefficients of p^0, p^1, p^2, \dots , the equation (17) is split as:

$$p^0 : \frac{d^2T_0}{dy^2} = 0 \tag{21}$$

$$p^1 : \frac{d^2T_1}{dy^2} = ST_0 - Br \left(\frac{du_0}{dy} \right)^2 \tag{22}$$

$$p^2 : \frac{d^2T_2}{dy^2} = ST_1 - 2Br \frac{du_0}{dy} \frac{du_1}{dy} \tag{23}$$

Additionally, transformed boundary conditions for momentum and energy equations are provided below.

$$u_0 = \Gamma \frac{du_0}{dy}, \quad u_1 = \Gamma \frac{du_1}{dy}, \quad u_2 = \Gamma \frac{du_2}{dy} \quad \text{at } y = 0 \tag{24}$$

$$u_0 = 0, \quad u_1 = 0, \quad u_2 = 0 \quad \text{at } y = 1$$

$$\frac{dT_0}{dy} = -B_{ii} [1 - T_0], \quad \frac{dT_1}{dy} = B_{ii} T_1, \quad \frac{dT_2}{dy} = B_{ii} T_2 \quad \text{at } y = 0 \tag{25}$$

$$T_0 = 0, \quad T_1 = 0, \quad T_2 = 0 \quad \text{at } y = 1$$

Solving for Eqn. (18) and Eqn. (21) we have:

$$u_0 = A_1y + A_2 \tag{26}$$

$$T_0 = B_1y + B_2 \tag{27}$$

Applying the boundary conditions for u_0 , and T_0 , respectively we have

$$u_0 = 0 \tag{28}$$

$$T_0 = \frac{B_{ii}}{(1+B_{ii})}(1-y) \tag{29}$$

From first order, we solve the Eqn. (18) and Eqn. (22) to have

$$T_1 = \left(\frac{SB_1y^3}{6} + \frac{SB_2y^2}{2} \right) + B_3y + B_4 \tag{30}$$

$$u_1 = \frac{y^2}{2} \frac{dp}{dx} - Gre \left(\frac{B_1y^3}{6} + \frac{B_2y^2}{2} \right) + A_3y + A_4 \tag{31}$$

where

$$A_3 = Gre \left(\frac{B_1}{6} + \frac{B_2}{2} \right) - \frac{1}{2} \frac{dp}{dx}, A_4 = \Gamma A_3, B_4 = \frac{SB_1}{6(1+B_{ii})} - \frac{SB_2}{2(1+B_{ii})}, B_3 = B_{ii} B_4 \quad (32)$$

For the second order, Eqn (20) and (23) are solved as

$$T_2 = S \left[\frac{SB_1 y^5}{120} + \frac{SB_2 y^4}{24} + \frac{B_3 y^3}{6} + \frac{B_4 y^2}{2} \right] + B_5 y + B_6 \quad (33)$$

$$u_2 = \left(M + \frac{1}{Da} \right) \left[\frac{y^4}{24} \frac{dp}{dx} - Gre \left(\frac{B_1 y^5}{120} + \frac{B_2 y^4}{24} \right) + \frac{A_3 y^3}{6} + \frac{A_4 y^2}{2} \right] - Gre \left[S \left(\frac{SB_1 y^5}{120} + \frac{SB_2 y^4}{24} \right) + \left(\frac{B_3 y^3}{6} + \frac{B_4 y^2}{2} \right) \right] + A_5 y + A_6 \quad (34)$$

where

$$B_6 = -S \left[\frac{SB_1}{120} + \frac{SB_2}{24} + \frac{B_3}{6} + \frac{B_4}{2} \right], B_5 = B_{ii} B_6 \quad (35)$$

$$A_5 = \frac{- \left(M + \frac{1}{Da} \right) \left[\frac{1}{24} \frac{dp}{dx} - Gre \left(\frac{B_1}{120} + \frac{B_2}{24} \right) + \frac{A_3}{6} + \frac{A_4}{2} \right] + Gre \left[S \left(\frac{SB_1}{120} + \frac{SB_2}{24} \right) + \left(\frac{B_3}{6} + \frac{B_4}{2} \right) \right]}{(1+\Gamma)} \quad (36)$$

$$A_6 = \Gamma A_5$$

Therefore, the approximate solutions for Eqs. (8) and (9) are:

$$u = u_0 + u_1 + u_2 + \dots \quad (37)$$

$$T = T_0 + T_1 + T_2 + \dots \quad (38)$$

The skin friction (Sk) on both the plates can be expressed as coefficient of surface skin stress is given below

$$Sk_{(0,1)} = \frac{du}{dy} \Big|_{(y=0,1)} \quad (39)$$

$$\frac{du}{dy} \Big|_{(y=0)} = (-Gre B_2 + A_3) + A_5 \quad (40)$$

$$\frac{du}{dy} \Big|_{(y=1)} = \left(A_3 + Gre \left(\frac{B_1}{6} + \frac{B_2}{2} \right) - \frac{1}{2} \frac{dp}{dx} \right) \quad (41)$$

$$+ \left(\left(M + \frac{1}{Da} \right) \left[\frac{1}{6} \frac{dp}{dx} - Gre \left(\frac{B_1}{24} + \frac{B_2}{6} \right) + \frac{A_3}{2} + A_4 \right] - Gre \left[S \left(\frac{SB_1}{24} + \frac{SB_2}{6} \right) + \left(\frac{B_3}{2} + B_4 \right) \right] \right)$$

while the rate of heat transfer which is expressed as local Nusselt number (Nu) at both the plates are given by:

$$Nu_{(0,1)} = \frac{dT}{dy} \Big|_{(y=0,1)} \quad (42)$$

$$\frac{dT}{dy} \Big|_{(y=0)} = B_2 + B_3 + B_5 \quad (43)$$

$$\frac{dT}{dy} \Big|_{(y=1)} = B_1 + B_2 + \left(\frac{SB_1}{2} + SB_2 + B_3 \right) + \left(S \left[\frac{SB_1}{24} + \frac{SB_2}{6} + \frac{B_3}{2} + B_4 \right] + B_5 \right) \quad (44)$$

(b) Numerical Solutions

Equations (5) and (6) subject to (7) are solved numerically using implicit finite difference method as in (45) and (46)

$$-r u_{i-1}^{j+1} + (1+2r) u_i^{j+1} - r u_{i+1}^{j+1} = (1-r_1) u_i^j + Gre \Delta t T_i^j + \lambda \Delta t \quad (45)$$

$$-r T_{i-1}^{j+1} + (Pr+2r) T_i^{j+1} - r T_{i+1}^{j+1} = (Pr-S \Delta t) T_i^j + r_2 (u_{i+1}^j - u_{i-1}^j)^2 \quad (46)$$

where

$$r = \frac{\Delta t}{(\Delta y)^2}, r_1 = \Delta t \left(M + \frac{1}{Da} \right), r_2 = \frac{Br}{4} \frac{\Delta t}{(\Delta y)^2}$$

4. Results and Discussion

A theoretical investigation is conducted to see the effects of Navier slip and convective boundary conditions on transient mixed convection flow of viscous dissipative fluid in a vertical channel. In graphs and tables, the regulating flow parameters' impacts are displayed. For discussion purposes, the values of the flow variables are carefully selected to reflect accurate characteristics of some fluid flow. The following default settings were used in this study with air as the working fluid:

($Gre = 50, S = 0.1, Br = 0.1, Pr = 0.71, M = 0.1, Da = 0.1, B_{ii} = 0.1, \Gamma = 0.1$) unless otherwise stated, while $S < 0$ and $S > 0$ denotes

the production and absorption of heat, respectively. The skin friction and the rate of heat transfer on the fluid-plate contact are tabulated in tables 1, 2, 3, 4 and 5 to present S, Br, Da, M and B_{ii} respectively.

The actions of Br on the velocity and temperature profiles are shown in Figures 2a and b, respectively. It is clear from 2a and b that an increase in Br raises the fluid temperature and velocity, respectively. The impact of the Darcy parameter (Da) and magnetic field (M) on the velocity profile is seen in Figures 3a and b. Figure 3a shows that a rise in M values results in a decrease in fluid flow velocity. Figure 3b demonstrates that the velocity rises with higher Darcy number values. The opposite is seen in the bottom section of the plate when the plate is cool. This is physically true because when flow material is transferred in large quantities, more viscous energy is created, increasing the barrier layer and thickness and boosting fluid velocity as a result. The effects of the mixed convection parameter (Gre) on the velocity profile are depicted in Figures 4a and b, respectively. The velocity profile rises significantly near to the heated plate when the mixed convection parameter is raised, as seen in Figure 4a, as thermal buoyancy forces rise, heat energy diffuses more easily, and the fluid becomes less dense, resulting in an increase in fluid flow. Additionally, it can be observed that when thermal buoyancy increases at $Gre > 0$, the thickness of the velocity profile boundary layers grows at the heated plate's top portion, with the opposite trend observed at the bottom portion. The physical manifestation of this is an increase in fluid flow velocity brought on by the energy released by viscous dissipation and heat carried by the heated plate; the opposite situation is shown in Figure 4b at $Gre < 0$. As can be shown in Figures 5a and b, temperature and velocity are significantly influenced by the Prandtl number (Pr). This is because increasing this parameter causes a decrease in the fluid's thermal conductivity, which decreases the rate at which heat is transferred from the heated channel walls into the fluid flow. Additionally, it is seen that the boundary layer thickness has an impact comparable to that of 5a and 5b. Figures 6a and 6b show the impact of heat Sink (S) on velocity and temperature profiles, respectively. In both figures, a considerable drop in velocity and temperature was seen as a result of an increase in heat absorption $S > 0$, indicating that Sink (S) decreases fluid flow temperature and velocity in this research. Figures 7a and 7b, demonstrating how the Biot (B_{ii}) number affects temperature and velocity profiles, respectively. It can be seen that when heat is introduced through the heated plate, the velocity and temperature profiles both rise noticeably. This is physically accurate since the porosity of the plates permits fluid flow across the system, which ultimately results in an increase in fluid motion. Additionally, the energy lost by diffusion into other parts of the system raises the fluid's temperature and velocity. . Figure 8 and 9 Illustrated the effect of Biot number B_{ii} on skin friction and the rate of heat transfer, it is evident from 8a that the skin friction increases as the values of B_{ii} increases at $y = 0$ and the reversed case is observed in 8b at $y = 1$, while in Figure 9a the fluid flow trends decreases as the values of B_{ii} increases at $y = 0$ and the opposite phenomenon is noticed in 9b at $y = 1$. Table 1. presents the effects of heat source/sink parameter (s) on the frictional force and the rate of heat transfer when other parameters are kept constant. It is physically seen that growing levels of heat source decreases the skin friction at $y = 0$ whereas the same phenomenon is recorded at the cold plate $y = 1$. Additionally, rate of heat transfer is enhanced at $y = 0$ while an oppose phenomenon occurs at $y = 1$. The influence of Br on shear stress and heat transfer rate is demonstrated on Table 2. As other parameters are maintained at constant values. Higher values of Br is seen to boost the skin friction at the heated part of the plate and cold plate at $y = 1$. Similarly, the rate of heat transfer is improved for rising levels of Br , whereas an opposite case is seen to occur at $y = 0$. Table 3. Depicts the impact of Darcy (Da) on the heated and cold plates ($y = 0$, and $y = 1$, respectively) when other parameters are taken constants values. It is clear that increasing values of Da leads to a dramatic increase in the frictional force at the plate $y = 0$, whereas at the cold plate, a reverse phenomenon is demonstrated. The effect of M when other parameters are kept constant, on the skin friction is displayed in table 4. It is obvious that greater values of M is seen to decrease the skin friction at the heated and at the cold plat ($y = 0$ and $y = 1$). The impact of the Biot (B_{ii}) number on skin friction and shear stress at the heated and cold plates is represented in table 5, it is noticed that skin friction and shear stress increases significantly with increase in the values of B_{ii} through the heated and cold plates. This is true, since the existence porosity of the plates, allows fluid flow through the system which at the end leads to increase in fluid motion and the energy dissipated diffuses to other part of the system which increases both skin friction and shear stress of fluids.

Table 1: Illustrates the effect of skin friction and Nusselt number at the hot and cold plate ($y = 0$ and $y = 1$) for heat source/sink parameter (S) at $Gre = 50$, $Br = 0.01$, $Da = 0.1$, $M = 1$, and $Pr = 0.71$

S	τ_0	τ_1	$Nu_0 (-)$	Nu_1
0.1	0.0024	0.2607	0.0364	0.0342
0.3	0.0021	0.2512	0.0365	0.0316
0.5	0.0019	0.2426	0.0365	0.0291
0.7	0.0017	0.2349	0.0366	0.0270

Table 2: Shows the effect of skin friction and Nusselt number at the hot and cold plate ($y = 0$ and $y = 1$ respectively) for Br at $S = 0.1$, $Gre = 50$, $Da = 0.1$, $M = 1$, $Pr = 0.71$, and $B_{ii} = 0.1$.

Br	τ_0	τ_1	$Nu_0 (-)$	Nu_1
1	0.0033	0.2871	0.0361	0.0482
3	0.0046	0.3244	0.0356	0.0698
5	0.0110	0.5273	0.0331	0.2246
7	0.0194	0.8304	0.0298	0.5569

Table 3: Shows the effect of skin friction at the hot and cold plate when $y = 0$ and $y = 1$, for Da at $S = 0.1$, $Gre = 100$, $B_{ii} = 0.1$, $M = 1$, $Br = 0.01$, $Pr = 0.71$.

Da	τ_0	τ_1
0.1	0.0023	0.2584
0.3	0.0082	0.4629
0.5	0.0109	0.5558
0.7	0.0125	0.6081

Table 4: Shows the skin friction at the hot and cold plate when $y = 0$ and $y = 1$ respectively, for M at $Gre = 100$, $B_{ii} = 0.1$, $S = 0.1$, $Br = 0.01$, $M = 1$, and $Pr = 0.71$

M	τ_0	τ_1
1	0.0023	0.2584
3	0.0016	0.2301
5	0.0010	0.2081
7	0.0005	0.1904

Table 5: Shows the effect of skin friction and Nusselt number at the hot and cold plate when $y = 0$ and $y = 1$ respectively, for B_{ii} at $S = 0.1$, $Gre = 50$, $Br = 0.01$, $Da = 0.1$, $M = 1$, $Pr = 0.71$.

B_{ii}	τ_0	τ_1	$Nu_0 (-)$	Nu_1
0.1	0.0024	0.2607	0.0364	0.0342
0.3	0.0026	0.4919	0.0928	0.0914
0.5	0.0031	0.6724	0.1339	0.1369
0.7	0.0038	0.8160	0.1649	0.1736

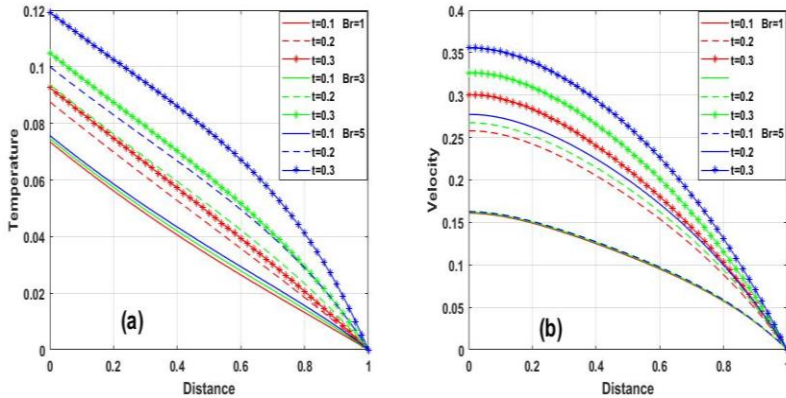


Figure 2: Illustration of Brinkman Number on Velocity and Temperature profiles ($Gre = 40$, $Da = 0.1$, $Mg = 1$, $S = 0.1$, $Pr = 0.71$, and $Br = 0.01$)

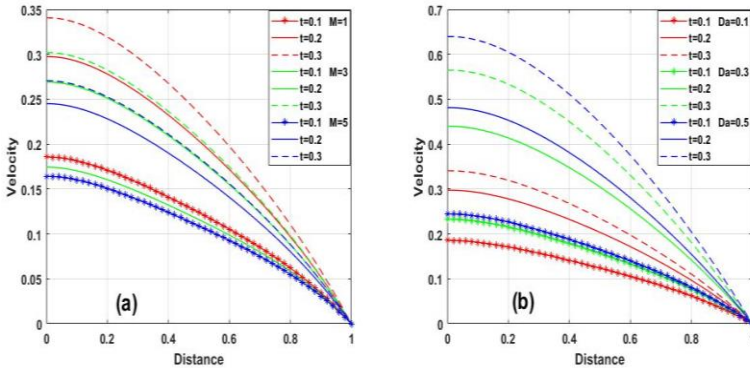


Figure 3:Effect of M and Da on velocity profile ($Gre = 50$, $Mg = 1$, $Br = 0.01$, $Pr = 0.71$)

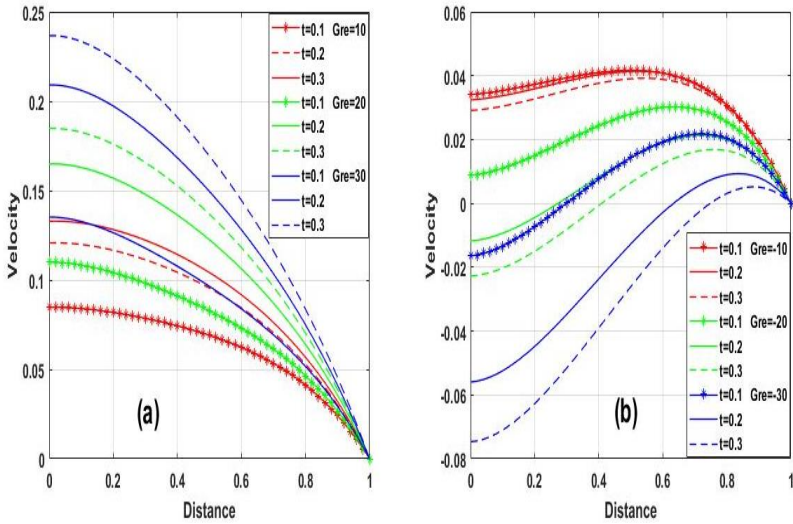


Figure 4: Effect of Mixed convection parameter (Gre) on velocity ($B_{ii} = 0.01, Da = 0.1, Mg = 1, S = 0.1, Pr = 0.71, \Gamma = 0.1$ and $Br = 0.01$)

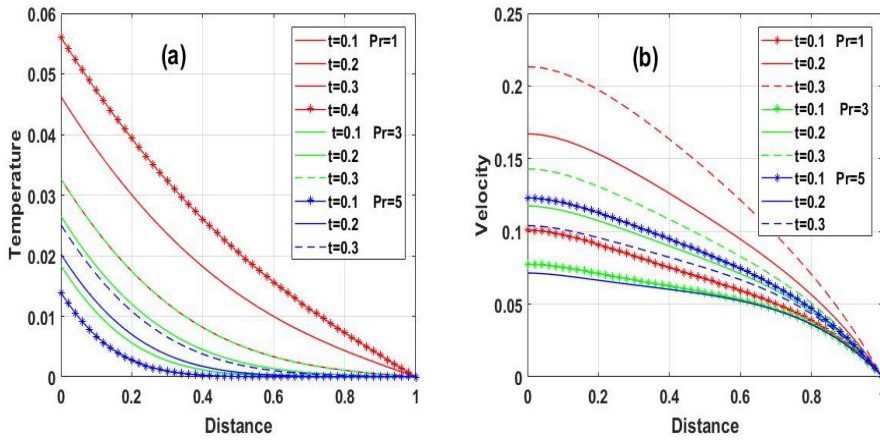


Figure 5: Presentation of Prandtl number on temperature and velocity profile ($Gre = 50, Da = 0.1, Mg = 1, S = 0.1, \Gamma = 0.1$ and $Br = 0.01, B_{ii} = 0.01$)

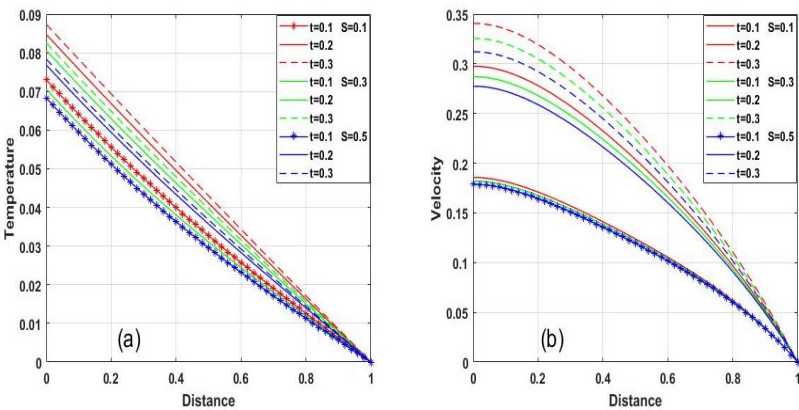


Figure 6: Effect of heat Sink (S) on temperature and velocity profile ($Gre = 40, Da = 0.1, Mg = 1, Pr = 0.71,$ and $Br = 0.01$)

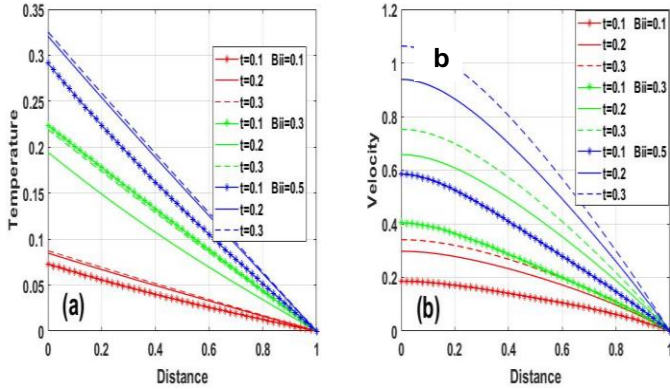


Figure 7: The result of temperature and velocity profile for Biot number (B_{ii}) ($Gre = 50, Da = 0.1, Mg = 1, S = 0.1, Pr = 0.71, \Gamma = 0.1$ and $Br = 0.01, B_{ii} = 0.01$)

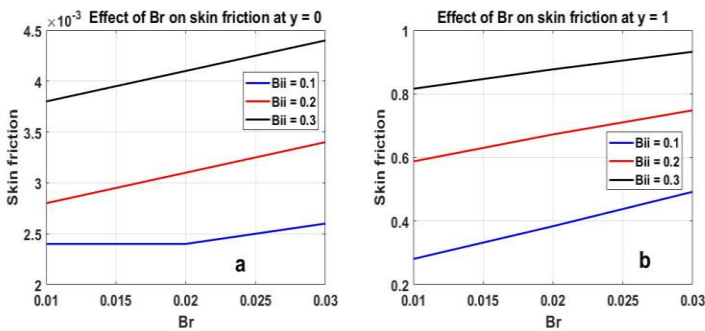


Figure 8: Effect of Biot Number on skin friction at $y = 0$ and $y = 1$ respectively

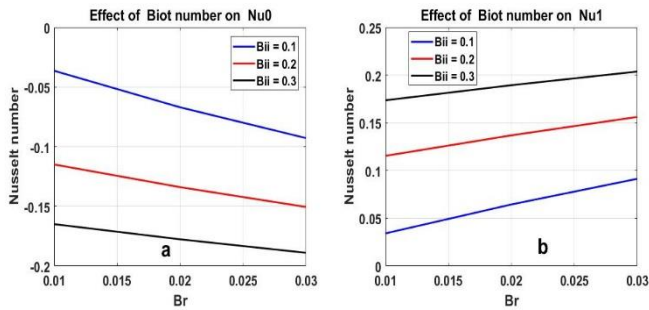


Figure 9: Effect of Biot number (B_{ii}) on rate of heat transfer (Nu) at $y = 0$ and $y = 1$ respectively

6. Conclusion

In this study, the effects of Navier slip and convective boundary conditions on transient mixed convection flow of viscous dissipative fluid in a vertical channel are investigated. The Homotopy perturbation method is used to get the steady state analytical solutions for energy, momentum, frictional forces, and heat transfer rate. The impact of dimensionless regulating parameters and dynamic flows is discussed and shown in graphs and tables after the time-dependent controlling equations are numerically solved using an implicit finite difference scheme. The main conclusions are summarized as follows:

- (i) The fluid velocity and temperature are improved by raising the values of Gre , Br , B_{ii} , and Da , whereas the flow pattern is negatively impacted by raising the values of S , M , and Pr .
- (ii) Heat transmission rates decrease as Br and S levels increase at $y = 0$ and $y = 1$ respectively.
- (iii) As the values of B_{ii} increase at $y = 0$ and $y = 1$ respectively, the rate of heat transfer and skin friction both improve.
- (iv) At $y = 0$ and $y = 1$, S and M lessen skin friction.

References

- [1] M Avci and O. Aydin, Mixed convection in a vertical parallel plate microchannel With Asymmetric Wall Heat Fluxes, (2017) *J. Heat Transfer*. 129, p. 1091–5.
- [2] A. Avramenko, A.I. Tyrinov, I.V. Shevchuk, N.P. Dmitrenko, A.V. Kravchuk, and I.V. Shevchuk. Mixed convection in a vertical flat microchannel, (2017) *Int J Heat Mass Transf.* 106, p. 1164–73.
- [3] B.K. Jha, S. Gabriel, and P.B. Malgwi, Adomian Decomposition Method for combined effect of Hall and ion-slip on mixed convection flow of chemically reacting Newtonian fluid in a micro-channel with heat absorption/generation (2020) *Int. J Modern Phys. C*. DOI: 10.1142/S0129183120501508.
- [4] K. Khanafera, M.S. Aithal, and K. Vafaid, Mixed convection heat transfer in a differentially heated cavity with two rotating cylinders, (2019) *Int. J Therm. Sci.* 135, p. 117–32.
- [5] V.G. Gupta, J. Ajay, and A. Kumar, Mixed Convection Flow of Viscous Dissipating Fluid through Channel Moving in Opposite Direction (2016) *IOSR Journal of Mathematics*. 12, p. 50-59
- [6] Z. Masoud, T. Davood and A. Karimipou, Developing a new correlation to estimate the thermal conductivity of MWCNT-CuO/water hybrid nanofluid via an experimental investigation (2017) *J. Therm Anal Calorim.* 129, p. 859–67.
- [7] H. Xu and Q. Sun. Generalized hybrid nanofluid model with the application of fully developed mixed convection flow in a vertical microchannel, (2019) *Commun Theor Phys.* 71, p. 903–11.
- [8] E. Manay and E. Mandev. Experimental investigation of mixed convection heat transfer of nanofluids in a circular microchannel with different inclination angles, (2019) *J. Therm Anal Calorim.* 135, p. 887–900.
- [9] B. Gebhart. Effect of viscous dissipation in natural convection, (1962) *J. Fluid Mech*, 14, p. 225 – 32.
- [10] O.A. Ajibade and M.U. Ayuba, Effects of viscous dissipation on a steady mixed convection Couette flow of heat generating/absorbing fluid, (2021a) *Journal of Pure and Applied Sciences*. 21, p. 67 – 7668.
- [11] O.A. Ajibade and M.U. Ayuba, An analytical study on effect of viscous dissipation and suction/injection on a steady MHD natural convection couette flow of heat generation/absorbing fluid, (2021b) *Advances in Mechanical Engineering*. 13, p. 1 – 12
- [12] B.K. Jha and O.A. Ajibade, Effect of viscous dissipation on natural convection flow between vertical parallel plates with time-periodic boundary conditions, (2012) *Commun Nonlin Sci Numer Simul.* 17, p. 1576–87.
- [13] B.K. Jha, D. Daramola and O.A. Ajibade, Mixed convection in an inclined channel filled with porous material having time-periodic boundary conditions: steady-periodic regime, (2015) *Trans Porous Media.* 2, p. 495–512.
- [14] O.A. Ajibade and U.O. Thomas, Entropy generation and irreversibility analysis due to steady mixed convection flow in a vertical porous channel (2017) *Int J. Heat Technol.* 35, p. 433–46.
- [15] A. Mohamed, Mixed convection flow of a micropolar fluid from an unsteady stretching surface with viscous dissipation. (2013) *J. Egypt Math Soc.* 21, p. 385–94.
- [16] A. Mohamed, Unsteady mixed convection heat transfer along a vertical stretching surface with variable viscosity and viscous dissipation, (2014) *J. Egypt Math Soci.* 22, p. 529–37.
- [17] P. Dulal and M. Hiranmony, Effects of temperature-dependent viscosity and variable thermal conductivity on MHD non-darcy mixed convective diffusion of species over a stretching sheet, (2014) *J. Egypt Math Soc.* 22, p. 123-133.
- [18] Y. Mahmoudi, K. Hooman, and K. Vafai, *Convective Heat Transfer in Porous Media*, (2020) (New York, USA: Taylor & Francis Group, LLC CRC Press).
- [19] S.K. Ahmad, Y. Bello and M.M Hamza, A numerical investigation of hydro-magnetic mixed convection flow of viscous dissipative fluid in a channel filled with porous material, (2023) *J. Trends in Science*. <https://doi.org/10.48048/tis.2024.6162>.
- [20] A.J. Chamkha, R.S. Gorla, and K. Ghodeswar, Non-similar solution for natural convective boundary layer flow over a sphere embedded in a porous medium saturated with a nano fluid, (2011) *Transp Porous Media.* 86(1), p. 13–22.
- [21] A.J. Chamkha, Mixed convection flow along a vertical permeable plate embedded in a porous medium in the

- presence of a transverse magnetic field,” Numerical Heat Transfer, Part A, Applications, (2007) An International Journal of Computation and Methodology. 34(1), p. 93–103.
- [22] B.J. Gireesha and S. Sindhu, MHD natural convection flow of casson fluid in an annular microchannel containing porous medium with heat generation/absorption, (2020) Nonlinear engineering. 9, 223-232.
- [23] A. Noor, P. Saykat, M.K. Enamul, S.H. Mohammad, L. Giulio, Transient MHD radiative fluid flow over an inclined porous plate with thermal and mass diffusion using numerical approach, (2021) 8(5), p. 739-749
- [24] JH He. Homotopy perturbation method for solving boundary value problems. (2006) Phys Lett A 350, p. 87–8.
- [25] MM Hamza. Free convection slip flow of an exothermic fluid in a convectively heated vertical channel, (2018) Ain Shams Engineering Journal, 9, 1313-1323.